


## Article

# An Analytical Investigation of Natural Convection of a Van Der Waals Gas over a Vertical Plate

Andriy A. Avramenko <sup>1</sup>, Igor V. Shevchuk <sup>2,\*</sup>  and Margarita M. Kovetskaya <sup>1</sup>

<sup>1</sup> Institute of Engineering Thermophysics, National Academy of Sciences, 03057 Kiev, Ukraine; aaav1@i.com.ua (A.A.A.); KovetskaMargarita@ukr.net (M.M.K.)

<sup>2</sup> Faculty of Computer Science and Engineering Science, TH Köln—University of Applied Sciences, 51643 Gummersbach, Germany

\* Correspondence: igor\_v.shevchuk@th-koeln.de

**Abstract:** The study focused on a theoretical study of natural convection in a van der Waals gas near a vertical plate. A novel simplified form of the van der Waals equation derived in the study enabled analytical modeling of fluid flow and heat transfer. Analytical solutions were obtained for the velocity and temperature profiles, as well as the Nusselt numbers. It was revealed that nonlinear effects considered by the van der Waals equation of state contribute to acceleration or deceleration of the flow. This caused respective enhancement or deterioration of heat transfer. Results for a van der Waals gas were compared with respective computations using an ideal gas model. Limits of the applicability of the simplified van der Waals equations were pinpointed.

**Keywords:** natural convection; van der Waals gas; fluid flow; heat transfer; Nusselt number; velocity profiles; temperature profiles



**Citation:** Avramenko, A.A.; Shevchuk, I.V.; Kovetskaya, M.M. An Analytical Investigation of Natural Convection of a Van Der Waals Gas over a Vertical Plate. *Fluids* **2021**, *6*, 121. <https://doi.org/10.3390/fluids6030121>

Academic Editors: Andrey Pototsky and Mehrdad Massoudi

Received: 26 February 2021

Accepted: 14 March 2021

Published: 15 March 2021

**Publisher's Note:** MDPI stays neutral with regard to jurisdictional claims in published maps and institutional affiliations.



**Copyright:** © 2021 by the authors. Licensee MDPI, Basel, Switzerland. This article is an open access article distributed under the terms and conditions of the Creative Commons Attribution (CC BY) license (<https://creativecommons.org/licenses/by/4.0/>).

## 1. Introduction

For most engineering applications of gases, the ideal gas model can be used with quite high accuracy. Applications that require using real-gas models are processes near the condensation point of gases, critical points, at very high pressures, etc. Hydrogen fuel tanks [1] or ethylene polymerization reactors [2] operate at high system pressure levels. Here, effects occur that cannot be described by an ideal gas model. For instance, gas density and the tank volume for the compressed gas cannot be estimated with sufficient accuracy. Tank filling can be simplified to a throttling valve where the Joule–Thomson effect occurs, which describes an adiabatic isenthalpic throttling accompanied with a drastic reduction of pressure and temperature [1]. Water vapor in steam power plants and refrigerant vapor in refrigerators also cannot be treated as ideal gases [3].

Experimental studies proved that the ideal-gas relation describes well behavior of real gases at relatively low densities. Many gases such as air, nitrogen, oxygen, hydrogen, helium, argon, neon, krypton, carbon dioxide, etc. can be treated as ideal gases with negligible error (often less than 1 percent) [3]. Superheated water vapor can be treated as an ideal gas, regardless of its temperature, at atmospheric pressure and below it. Higher pressures require higher temperatures for the ideal-gas model to be valid (to ensure relatively low vapor densities). Otherwise the ideal gas model at higher pressures yields unacceptable errors (even over 100 percent), especially in the vicinity of the critical point and the saturated vapor line [3]. Water vapor in the humid atmospheric air complies with an ideal gas in air-conditioning applications. However, in steam power plants, working pressures are very high, so that instead of ideal-gas relations engineers and researchers deal with diagrams or tables presenting properties of water vapor as a real gas [3].

The limits of applicability of the ideal gas model for air are low densities (large specific volumes  $\nu$ ), low pressures (<10 bar), and moderate/high temperatures (up to 600 °C) [4].

One way to account for the deviation from ideal-gas behavior at a given temperature and pressure is the introduction of the compressibility factor  $Z$  defined as [3]:

$$Z = \frac{p}{RT\rho} = \frac{pv}{RT} = \frac{pV}{mRT} \quad (1)$$

For ideal gases,  $Z = 1$ , which yields the known ideal-gas equation [3,4]

$$pV = m \frac{R_m}{M_i} T, \quad pV = nR_m T, \quad pv = \frac{R_m}{M_i} T = RT \quad (2)$$

where  $n = m/M_i$  is the number of moles.

For real gases,  $Z$  can be greater than or less than unity [3]. Temperatures and pressures of real gases can be normalized with respect to their critical temperatures and pressures

$$p_R = \frac{p}{p_{cr}}, \quad T_R = \frac{T}{T_{cr}} \quad (3)$$

where  $p_R$  is the reduced pressure and  $T_R$  is the reduced temperature. According to the principle of corresponding states, the  $Z$  factor for all gases is approximately the same at the same reduced pressures and temperatures. Experimentally determined  $Z$  values are presented in [3] in a graphical form. The diagram indicates that (a) at very low pressures ( $p_R \ll 1$ ), gases behave as an ideal gas regardless of temperature, (b) at high temperatures ( $T_R > 2$ ), gases behave as an ideal gas regardless of pressure (except for  $p_R \gg 1$ ), (c) the deviation from ideal-gas model is greatest in the vicinity of the critical point [3].

In many cases, it is desirable to deal with more accurate and elaborate equations of state (rather than diagrams or tables) that perform accurately over a larger region than the ideal gas law. Among them, the van der Waals equation is one of the most known and widely used. Three forms of this equation are employed in practice [3–7]:

$$\left(p + n^2 \frac{a_*}{V^2}\right)(V - nb_*) = nR_m T, \quad (4)$$

$$\left(p + n^2 \frac{a_*}{V_m^2}\right)(V_m - nb_*) = R_m T, \quad (5)$$

$$\left(p + \frac{a}{v^2}\right)(v - b) = RT \quad (6)$$

where  $V_m = V/m = M_i/\rho$  is molar volume, whereas  $R = R_m/M_i$  and  $R_m = 8314 \text{ J}/(\text{mol}\cdot\text{K})$ .

The first and the second derivatives of  $p$  with respect to  $v$  at the critical point must be zero, which yields [5–7]

$$p_R = \frac{a_*}{27b_*^2}, \quad T_R = \frac{8a_*}{27R_m b_*}, \quad (7)$$

$$a = 3p_{cr}v_{cr}^2, \quad b = \frac{v_{cr}}{3}, \quad Z_{cr} = \frac{p_{cr}v_{cr}}{RT_{cr}} = \frac{3}{8}, \quad (8)$$

$$a = \frac{a_*}{M_i^2}, \quad b = \frac{b_*}{M_i} \quad (9)$$

Experimental values of the compressibility factor  $Z_{cr}$  for real gases are equal to  $Z_{cr} = 0.2\text{--}0.3$ . To further increase the accuracy of the van der Waals equation of state, the values of the constants  $a$  and  $b$  are selected via comparisons with experiments for real gases over a wider range instead of a single point [5–7].

Many problems of natural and mixed (natural and forced) convective heat transfer were studied in the literature, which arise from numerous industrial applications [8–10]. However, the most widespread modeling approach to them deals with the fluids with constant physical properties or with density described by the ideal-gas Equation (2).

Strong thermodynamic effects of real gases, which cannot be described by the ideal gas equation, also have a significant effect on the processes of flow, heat transfer, and mass transfer of gases in industrial equipment. Several authors have used the van der Waals equation to model the thermodynamic state of a real gas in a number of engineering applications.

The special properties of fluids near the thermodynamic critical point are used in power and aerospace engineering [11,12]. Much attention is paid to modeling of heat transfer processes in the region of nonlinear dependence of density of gaseous coolants on temperature described by the van der Waals equation of state.

Thermogravitational convection in a horizontal layer of a compressible van der Waals gas heated from below was studied by Gorbunov et al. [11]. They revealed conditions for the onset of the Rayleigh-Bénard convection and considered characteristics of convective heat transfer, as well as the reasons for its deterioration because of hydrodynamic stability. The Rayleigh-Bénard convection near the threshold of the onset of stability of near-critical fluids described by Navier-Stokes equations together with the van der Waals equation of state was also considered in the works [12–14]. They determined limiting values of the Rayleigh number near the thermodynamic critical point of helium and demonstrated effects of compressibility in near-critical fluids on steady-state convection beyond the stability threshold.

Laminar free convection of a van der Waals supercritical fluid near a vertical heated plate was simulated numerically in [15]. Here the effect of wall temperature inhomogeneity on heat transfer was in main focus. Turbulent Rayleigh-Bénard convection in a van der Waals supercritical fluid confined in a cubic cell heated from below was considered in [16]. The authors identified vortex structures in the computational domain, computed Nusselt number distributions on horizontal walls, and compared their results with the ideal gas model at the same Rayleigh numbers.

Heat transfer in two-phase flows of van der Waals fluids was studied in [17–20]. Free Rayleigh-Bénard convection was numerically investigated in [17]. The mathematical model [17] was able to describe liquid-vapor phase transitions. Phase separation in convective flow of a van der Waals fluid with varying temperature was investigated in [18]. An approach to modeling of a boiling van der Waals liquid based on the diffusive representation of the phase interface was suggested in [19]. Complex hydrodynamic processes with evaporation and condensation were numerically simulated in [20]. The authors demonstrated evolution of bubbles in the modes of nucleate and film boiling depending on the wettability of the heated surface.

Results of numerical simulation of phase separation in a van der Waals liquid are presented in [21]. The authors depicted spinodal decomposition for the critical state of a liquid and compared results of two- and three-dimensional modeling. Marangoni convection caused by the temperature gradient in the mixture of a liquid and a van der Waals gas was modeled in [22].

A study and a comparative analysis of the conditions of the onset of filtration convection in an ideal gas and a van der Waals gas in a horizontal porous layer was performed in the work [23]. Adiabatic heating and convection in a porous medium filled with a near-critical fluid was studied in [24]. The authors considered a problem of heat transfer in horizontal rectangular cells consisting of two porous layers heated from below with different porosities and demonstrated emergence and development of convective structures in the computational domain.

To conclude, the overview of the studies devoted to mathematical modeling of heat transfer processes in fluids with a nonlinear dependence of density on temperature presented above revealed that heat transfer coefficients and critical Rayleigh numbers strongly depend on the effects of compressibility of the medium. All authors used the van der Waals model of a real gas in the form of either of Equations (4)–(6). Because of its relative mathematical complexity, this model enables performing only numerical, but not analytical, modeling of the transport processes. Therefore, the objective of the present work was a study of the influence of thermophysical properties of a van der Waals gas on heat

transfer during natural convection near a heated vertical plate. Special attention was paid to interpretation of the effects of the parameters in the van der Waals model on the fluid flow and heat transfer pattern due to varying density in comparison with the ideal gas model. A novel simplified form of the van der Waals equation derived in the present study enabled analytical modeling of fluid flow and heat transfer. Limits of the applicability of the simplified van der Waals equation were pinpointed and discussed. This all constitutes the novelty of the present investigation.

## 2. Mathematical Model

Let us consider steady-state natural convection near a vertical heated plate placed in a large volume of resting gas with a constant temperature  $T_\infty$ . The temperature of the heated plate  $T_w$  is also constant. For definiteness, we will assume that  $T_w > T_\infty$ . The results obtained here will be also valid for the case  $T_\infty > T_w$ . A lifting motion of a heated layer of a gas with the thickness  $\delta$  will arise near the plate. Let us place the origin of coordinates at the lower edge of the plate, direct the  $x$  axis in the streamwise direction of the moving gas layer, whereas the  $y$  axis will be normal to the surface of the plate (Figure 1). We will consider here a two-dimensional case and assume that the plate is infinite in the  $z$ -direction.

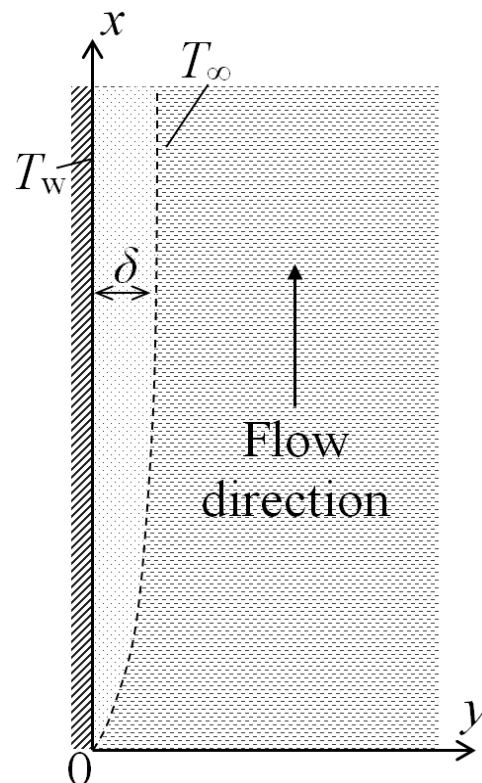


**Figure 1.** Schematic of two-dimensional natural convection near a heated vertical wall:  $x$ —flow direction,  $y$ —normal direction,  $\delta$ —boundary layer thickness,  $T_w$ —wall temperature,  $T_\infty$ —temperature outside of the boundary layer.

To solve the stated problem, let us make the following assumptions:

- (1) Inertial forces are negligible compared to gravitational and viscous forces;
- (2) Convective/conductive heat transfer in the streamwise direction is neglected;
- (3) The pressure gradient is zero;
- (4) All physical properties of the gas (excluding density) are constant.

As said above, our objective is to look into the effects of the van der Waals equation of state on the modeling of natural convection and compare it with the case where natural convection is simulated using the ideal-gas equation of state. Therefore, as a basis for the

comparisons, we will take the results of solving the problem for the ideal gas obtained in [25] based on a simplified model. According to [25], we will assume that the temperature in the moving gas layer is described by the equation

$$\theta = \theta_w \left(1 - \frac{y}{\delta}\right)^2, \tag{10}$$

where

$$\theta = T - T_\infty, \theta_w = T_w - T_\infty \tag{11}$$

The thickness of the moving gas layer  $\delta$  varies (grows) with height and depends on the flow velocity. Considering the above assumptions, we can write the equation of motion (i.e., momentum equation) in the following form:

$$\mu \frac{d^2 u}{dy^2} = -g(\rho_\infty - \rho) \tag{12}$$

The no-slip boundary condition on the wall is a standard one for usual internal/external flows (i.e., not microchannel flows).

The boundary conditions on the wall and on the boundary of the moving gas layer look as follows:

$$u = 0, \text{ for } y = 0 \text{ and } y = \delta \tag{13}$$

Equation (12) with boundary conditions (13) will be solved using the van der Waals equation of state (6) rewritten using gas density  $\rho$  instead of specific volume  $v$ :

$$\left(p + a\rho^2\right)\left(\frac{1}{\rho} - b\right) = RT, \tag{14}$$

where  $a$  and  $b$  are the van der Waals constants.

### 3. Analytical Solution

Let us rewrite the equation of motion (12) in a dimensionless form

$$\frac{d^2 U}{d\eta^2} = -\left(1 - \frac{\rho}{\rho_\infty}\right), \tag{15}$$

where

$$U = \frac{u\mu}{g\rho_\infty\delta^2}, \quad \eta = \frac{y}{\delta} \tag{16}$$

In this case, the boundary conditions (13) take the form

$$U = 0, \text{ for } \eta = 0 \text{ and } \eta = 1 \tag{17}$$

To solve Equation (15) with boundary conditions (17), it is necessary to mathematically express fluid density. At first, let us present Equation (14) in the following dimensionless form

$$\left(Z + \frac{Wa_a}{Z}\right)\left(1 - \frac{Wa_b}{Z}\right) = 1, \tag{18}$$

where

$$Wa_a = \frac{ap}{R^2T^2}, \quad Wa_b = \frac{bp}{RT} \tag{19}$$

are van der Waals numbers, respectively. Similar dimensionless criteria were introduced also in the work [15]. However, our results cannot be compared with the data of the authors [15], because they focused on the supercritical thermodynamic region [15].

Now we will solve Equation (18) with respect to the compressibility factor  $Z$ . This is a cubic equation that has two complex conjugate roots and one real root

$$Z(Wa_a, Wa_b) = \frac{1}{6} \left( \begin{aligned} & 2(1 + Wa_b) + \left( 2^{4/3} (-3Wa_a + (1 + Wa_b)^2) \right) / \\ & \left( \frac{2 + 6Wa_b + 6Wa_b^2 + 2Wa_b^3 + 9Wa_a(-1 + 2Wa_b) +}{3^{3/2} \sqrt{Wa_a(4Wa_a^2 + 4Wa_b(1 + Wa_b)^3 + Wa_a(-1 - 2\theta Wa_b + 8Wa_b^2))}} \right)^{1/3} + \\ & 2^{2/3} \left( \frac{2 + 6Wa_b + 6Wa_b^2 + 2Wa_b^3 + 9Wa_a(-1 + 2Wa_b) +}{3^{3/2} \sqrt{Wa_a(4Wa_a^2 + 4Wa_b(1 + Wa_b)^3 + Wa_a(-1 - 2\theta Wa_b + 8Wa_b^2))}} \right)^{1/3} \end{aligned} \right), \quad (20)$$

Equation (20) is rather cumbersome and difficult to use when integrating Equation (15). Therefore, let us simplify Equation (20) in the approximation of small values of the parameters  $Wa_a$  and  $Wa_b$ . For this purpose, we will expand Equation (20) in the Maclaurin series. We restrict ourselves to three terms of the series, which yields as a result

$$Z^{-1} = 1 + Wa_a - Wa_b, \quad (21)$$

or in the dimensional form

$$\rho = \frac{p}{RT} - \frac{bp^2}{R^2T^2} + \frac{ap^2}{R^3T^3} \quad (22)$$

We will perform validation of the simplified van der Waals equation of state (22) for ethylene. This gas has the following values of the parameters in the critical point and the constants  $a^*$  and  $b^*$  in the van der Waals Equations (4) and (5) [5–7]

$$\begin{aligned} R &= 296.4 \frac{\text{J}}{\text{kg}\cdot\text{K}}, \quad T_{cr} = 284.4\text{K}, \quad p_{cr} = 51.2\text{bar}, \quad M_i = 28 \frac{\text{kg}}{\text{kmol}}, \\ V_{m,cr} &= 0.1242 \frac{\text{m}^3}{\text{kmol}}, \quad a^* = 4.612 \frac{\text{bar}\cdot\text{L}^2}{\text{mol}^2}, \quad b^* = 0.0582 \frac{\text{L}}{\text{mol}} \end{aligned} \quad (23)$$

The constants  $a^*$  and  $b^*$  must be recalculated in the form of the constants  $a$  and  $b$  (and SI units) using Equation (9) to be further used in Equations (22) and (23).

$$a = \frac{a^*}{M_i^2} = 588.3 \frac{\text{Pa}\cdot\text{m}^6}{\text{kg}^2}, \quad b = \frac{b^*}{M_i} = 0.002079 \frac{\text{m}^3}{\text{kg}} \quad (24)$$

Curves of the gas density computed based on the ideal gas Equation (2), van der Waals Equation (5), and the simplified van der Waals Equation (22) are plotted in Figure 2 for undercritical superheated ethylene. It is evident that Equation (22) is more accurate than the ideal gas Equation (2) and agrees well with the van der Waals Equation (5) up to the pressure of  $p = 40$  bar (or  $p/p_{cr} = 0.4$ ) and  $T = T_{cr}$ . The relative inaccuracy of Equation (22) is about 8%, whereas the relative inaccuracy of Equation (2) is 22.7%.

For these values of the pressure and temperature, the values of both van der Waals numbers for ethylene are  $Wa_a = 2.78 \times 10^{-6}$  and  $Wa_b = 9.03 \times 10^{-7}$ . This justifies the assumption of the small values of the parameters  $Wa_a$  and  $Wa_b$  used to derive the simplified van der Waals Equation (22) in the form of Maclaurin series.

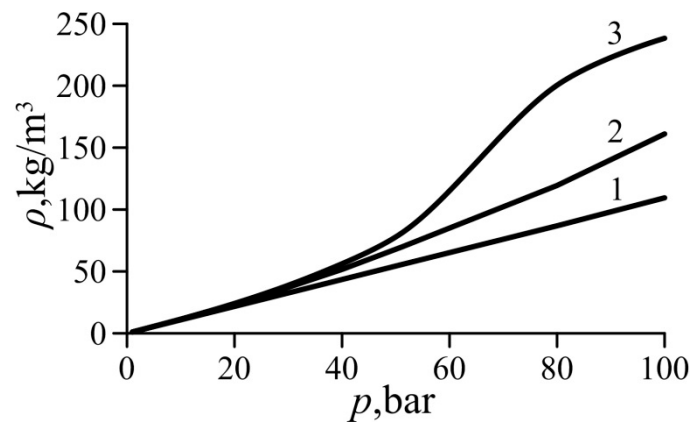


**Figure 2.** Gas density variation with pressure for ethylene. 1—Equation (2) (ideal gas), 2—Equation (22) (simplified van der Waals equation, present study), 3—Equation (5) (van der Waals equation).

Now we can express the ratio of densities  $\rho/\rho_\infty$  in Equation (15) using Equation (21). As a result, we get

$$\frac{d^2U}{d\eta^2} = - \left( 1 - \frac{Z}{1 + \beta\theta} \left( 1 - \frac{Wa_b}{1 + \beta\theta} + \frac{Wa_a}{(1 + \beta\theta)^2} \right) \right), \tag{25}$$

where the compressibility factor  $Z$  and van der Waals numbers are based on the parameters at the outer edge of the boundary layer, and

$$\beta = \frac{1}{T_\infty}. \tag{26}$$

Taking into account the simplified van der Waals Equation (22) and using Equation (1), it is possible to integrate Equation (25) twice with boundary conditions (17). For the convenience of further calculations, we represent the solution of Equation (25) in the following form:

$$\begin{aligned} W(\eta, \beta\theta_w, Wa_a, Wa_b) &= \frac{U(\eta, \beta\theta_w, Wa_a, Wa_b)}{\beta\theta_w} = \\ &= \frac{\left( \frac{Wa_a(1 + \beta\theta_w(-1 + \eta))}{1 + Wa_a + Wa_b} - 4(1 + \beta\theta_w(-1 + \eta)^2) \right) (-1 + \eta)\eta}{8\beta\theta_w(1 + \beta\theta_w)(1 + \beta\theta_w(-1 + \eta)^2)} + \\ &+ \frac{(-1 + \eta) \left( (8 + 3Wa_a - 4Wa_b)\sqrt{\beta\theta_w} (\arctan(\sqrt{\beta\theta_w}) + \arctan(\sqrt{\beta\theta_w}(-1 + \eta))) - 4\ln(1 + \beta\theta_w) \right)}{8\beta^2\theta_w^2(1 + Wa_a - Wa_b)} \\ &- \frac{4\ln(1 + \beta\theta_w(-1 + \eta)^2)}{8\beta^2\theta_w^2(1 + Wa_a - Wa_b)} \end{aligned} \tag{27}$$

To make sure that this solution is correct, let us find the limit of Equation (27) at  $\beta\theta_w \rightarrow 0$  for  $Wa_a = Wa_b = 0$  or, in other words, for an ideal gas. This yields

$$\lim_{\beta\theta_w \rightarrow 0} W(\eta, \beta\theta_w, 0, 0) = \frac{3\eta - 6\eta^2 + 4\eta^3 - \eta^4}{12}, \tag{28}$$

which corresponds to the velocity profile in the work [25].

Further, we will need to find the flow velocity averaged across the width of the free convective gas layer. The dimensionless average velocity is given by the equation

$$\begin{aligned} W_m(\beta\theta_w, Wa_a, Wa_b) &= (3(Wa_a - 4(2 + Wa_b))(1 + \beta\theta_w)\arctan(\sqrt{\beta\theta_w}) + \\ &+ \sqrt{\beta\theta_w}(-4(-6 + Wa_b(-3 + \beta\theta_w) - \beta\theta_w)(1 + \beta\theta_w) + Wa_a(-3 - 2\beta\theta_w + 4\beta\theta_w^2) - \\ &- 12(1 + \beta\theta_w)\ln(1 + \beta\theta_w))) / (48(1 + Wa_a - Wa_b)\beta\theta_w^{5/2}(1 + \beta\theta_w)) \end{aligned} \tag{29}$$



For the purpose of validation, for an ideal gas at  $\beta\theta_w \rightarrow 0$ , we obtain

$$\lim_{\beta\theta_w \rightarrow 0} W_m(\beta\theta_w, 0, 0) = \frac{1}{40}, \tag{30}$$

which conforms correctness of the solution (28).

When determining the gas mass flowrate (per unit length in the z-direction) through the cross section of a free convective layer with a thickness of  $\delta$ , we assume that a gas with a density  $\rho_\infty$  is entrained into the moving layer and acquires the mean integral velocity  $u_m$ , i.e.,

$$dG = d(\rho_\infty \delta u_m) = d\left(\frac{g\rho_\infty^2 \delta^3 \beta\theta_w W_m}{\mu}\right) = 3\frac{g\rho_\infty^2 \delta^2 \beta\theta_w W_m}{\mu} d\delta \tag{31}$$

In the moving free convective layer, the temperature of the gas varies non-linearly from  $T_w$  to  $T_\infty$ . On average, gas is heated to the average excess temperature of  $\theta_m = T_m - T_\infty$  (see Equation (11)). This requires heat supply with the rate

$$dQ = c_p \theta_m dG = h\theta_w dx = \frac{2k}{\delta} \theta_w dx, \tag{32}$$

where

$$\theta_m = \int_0^1 \theta d\eta = \frac{\theta_w}{3} \tag{33}$$

Equation (32) uses the relation between the heat transfer coefficient and thermal conductivity

$$h = \frac{2k}{\delta}, \tag{34}$$

which follows from the temperature distribution (10).

Taking into account Equations (30) and (33), we rewrite Equation (32) in the following form:

$$dx = \frac{c_p g \rho_\infty^2 \delta^3 \beta\theta_w W_m}{2\mu k} d\delta \tag{35}$$

Integration of Equation (35), provided that  $\delta = 0$  at  $x = 0$ , gives

$$\delta^4 = \frac{320\mu k}{c_p g \rho_\infty^2 \beta\theta_w (40W_m)} x \tag{36}$$

or

$$\delta = \sqrt[4]{\frac{320\mu k x}{c_p g \rho_\infty^2 \beta\theta_w}} \sqrt[4]{\frac{1}{40W_m}} = \frac{\delta_0}{\sqrt[4]{40W_m}}, \tag{37}$$

where  $\delta_0$  is the thickness of the moving fluid layer for an ideal gas at  $\beta\theta_w \rightarrow 0$ ,  $Wa_a = Wa_b = 0$  [15]. Based on Equation (34) one can find

$$h = \frac{2k}{\delta} = \frac{2k}{\delta_0} \sqrt[4]{40W_m} = h_0 \sqrt[4]{40W_m}, \tag{38}$$

where  $h_0$  is the heat transfer coefficient for an ideal gas. In dimensionless form, according to Equation (38), we obtain

$$\frac{h}{h_0} = \frac{hx/k}{h_0 x/k} = \frac{Nu}{Nu_0} = \sqrt[4]{40W_m}, \tag{39}$$

where  $Nu$  and  $Nu_0$  are the Nusselt numbers for van der Waals and ideal gas, respectively.



#### 4. Results and Discussion

Figures 3 and 4 show the effect of the van der Waals numbers on the velocity profiles. The values of these numbers are not bound to any gas and selected just to undertake a parametrical study of the effects that occur in real gases. As can be seen, an increase in both van der Waals numbers in the real gas model causes an increase in the local velocity. Consequently, the average velocity also increases. Let us recall that parameter  $a$  characterizes the additional pressure in the real gas (in comparison with an ideal gas) arising in the near-wall layer. Obviously, this effect increases the lift force. As a result, the velocity in the boundary layer increases.

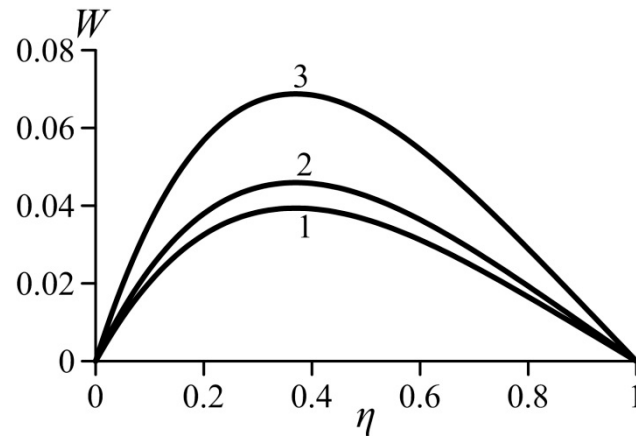


**Figure 3.** Effect of the van der Waals number  $Wa_a$  on the velocity profiles,  $\beta\theta_w = 0.01$ . 1—ideal gas ( $Wa_a = Wa_b = 0$ ), 2— $Wa_a = 0.1$  ( $Wa_b = 0.02$ ), 3— $Wa_a = 0.6$  ( $Wa_b = 0.02$ ).

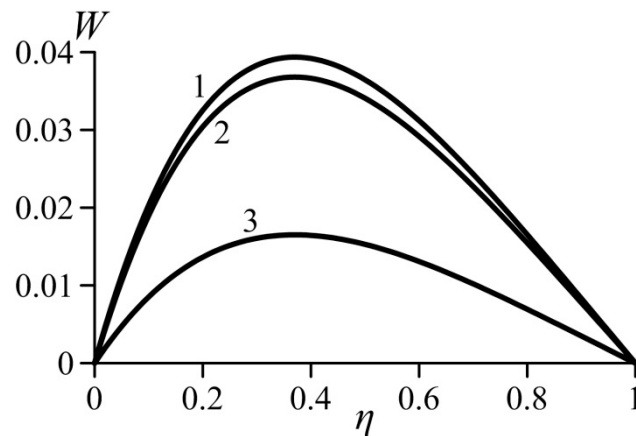


**Figure 4.** Effect of the van der Waals number  $Wa_b$  on the velocity profiles,  $\beta\theta_w = 0.01$ . 1—ideal gas ( $Wa_a = Wa_b = 0$ ), 2— $Wa_b = 0.1$  ( $Wa_a = 0.02$ ), 3— $Wa_b = 0.4$  ( $Wa_a = 0.02$ ).

As it is known, the parameter  $b$  describes an additional volume of space that is not filled with molecules. An increase in this additional volume and, therefore, in the parameter  $b$ , causes a decrease in the Archimedes force and decrease in the flow velocity.

An analysis of the solution for the velocity profile shows that the local velocity in the form of Equation (27) is self-similar with respect to the dimensionless product  $\beta\theta_w$ . Thus, for the same values of  $Wa_a$  and  $Wa_b$ , the velocity profiles (27) for all values  $\beta\theta_w$  collapse in a single curve.

The same is true for the case  $\beta\theta_w \rightarrow 0$ . For this case, one can find the limit

$$\lim_{\beta\theta_w \rightarrow 0} W(\eta, \beta\theta_w, Wa_a, Wa_b) = \frac{1+3Wa_a-2Wa_b}{1+Wa_a-Wa_b} \frac{3\eta-6\eta^2+4\eta^3-\eta^4}{12} = \frac{1+3Wa_a-2Wa_b}{1+Wa_a-Wa_b} W_0 \quad (40)$$

where  $W_0$  is the dimensionless velocity profile for an ideal gas. As mentioned above, all dimensionless velocity profiles are the same for different values of the parameter  $\beta\theta_w$ , including the case  $\beta\theta_w \rightarrow 0$ . Therefore, we can conclude that profile (40) coincides with profile (27). Consequently, profile (40) is universal and valid for all values of the parameter  $\beta\theta_w$ .

Similarly, we can find the limit for the average velocity (29). As a result, we have

$$\lim_{\beta\theta_w \rightarrow 0} W_m(\beta\theta_w, Wa_a, Wa_b) = \frac{1}{40} \frac{1+3Wa_a-2Wa_b}{1+Wa_a-Wa_b} = \frac{1+3Wa_a-2Wa_b}{1+Wa_a-Wa_b} W_{m0} \quad (41)$$

where  $W_{m0}$  is the dimensionless average velocity for an ideal gas. This expression is also valid for all values of the parameter  $\beta\theta_w$ .

Figures 5 and 6 show variation of the normalized Nusselt number  $Nu/Nu_0$  (or normalized heat transfer coefficient) as a function of the van der Waals numbers. These data were computed based on Equation (39). They practically coincide with the results obtained using Equation (39) together with Equation (29) for the average velocity. As expected, an increase in the parameter  $Wa_a$  causes heat transfer augmentation. At the same time, an increase in the parameter  $Wa_b$  yields heat transfer deterioration. This follows from the trend of the influence of the van der Waals numbers on the velocity profiles (Figures 3 and 4).

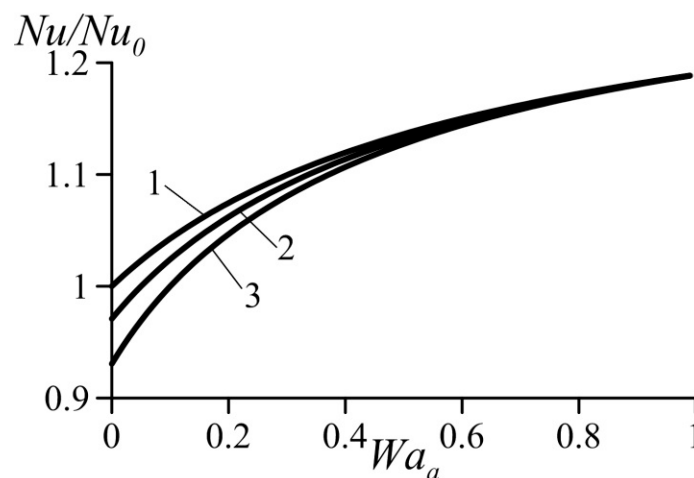


**Figure 5.** Effect of van der Waals number  $Wa_a$  on the normalized Nusselt number under condition  $Wa_b = \text{const}$ . 1— $Wa_b = 0$ , 2— $Wa_b = 0.1$ , 3— $Wa_b = 0.2$ .

As shown above, an increase in the dimensionless number  $Wa_a$  causes acceleration of the flow in the near-wall layer accompanied with heat transfer enhancement. An increase in the dimensionless number  $Wa_b$  causes deceleration of the flow in the near-wall layer accompanied with reduced heat transfer rates. Thus, heat transfer enhancement is caused by the effects taken into account by the van der Waals equation of state and neglected by the ideal-gas equation.

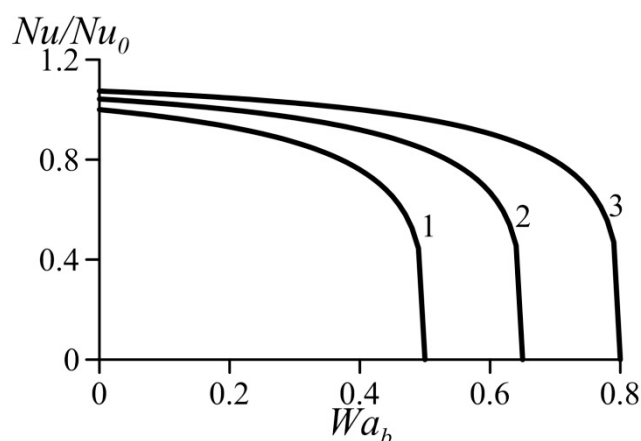


**Figure 6.** Effect of van der Waals number  $Wa_b$  on the normalized Nusselt number under condition  $Wa_a = \text{const.}$  1— $Wa_a = 0$ , 2— $Wa_a = 0.1$ , 3— $Wa_a = 0.2$ .

Now Equation (39) can be written in the following form

$$\frac{Nu}{Nu_0} = \sqrt[4]{\frac{1 + 3Wa_a - 2Wa_b}{1 + Wa_a - Wa_b}} \quad (42)$$

It follows also from Figures 5 and 6 that the effect of  $Wa_b$  is somewhat stronger than that of the  $Wa_a$ .

In addition, it can be seen that for certain combinations of the parameters  $Wa_a$  and  $Wa_b$ , an increase in the parameter  $Wa_b$  causes a sharp decrease in the heat transfer coefficient.

## 5. Conclusions

The problem of steady-state natural convection of a van der Waals gas near a vertical heated plate was considered. A novel simplified form of the van der Waals equation derived here enabled an analytical solution of the fluid flow and heat transfer problem. Limits of the applicability of the simplified van der Waals equations were estimated. Effects of the van der Waals equation of state on convective heat transfer were investigated, and the results were compared also with the case of an ideal gas. It was shown that nonlinear effects in the equation of state of the gas described by the parameter  $Wa_a(a)$  contribute to an increase in the velocity in the near-wall layer in comparison with an ideal gas. This is due to the effect of additional pressure characterized by the parameter  $a$  in the van der Waals equation. The effect of additional volume characterized by the parameter  $Wa_b(b)$  reduces the Archimedean force and decelerates the flow. The augmentation and weakening of heat transfer are caused also by the effects of nonlinearity in the van der Waals equation of state. This fact naturally follows from the trends of the effects of the van der Waals numbers on the velocity profiles.

**Author Contributions:** Analytical investigation, A.A.A.; conceptualization, A.A.A. and I.V.S.; methodology, A.A.A. and I.V.S.; validation and formal analysis, A.A.A., I.V.S., and M.M.K.; writing—original draft preparation, review and editing, A.A.A., I.V.S., and M.M.K.; writing of the final manuscript, A.A.A. and I.V.S. All authors have read and agreed to the published version of the manuscript.

**Funding:** The research contribution of A.A.A. and M.M.K. was funded via the program of research grants of the NAS of Ukraine “Support of priority for the state scientific researches and scientific and technical (experimental) developments” 2020–2021. Project 1.7.1.892: “Development of scientific and technical fundamentals of heat of mass transfer intensification in porous media for materials of building designs and the thermal engineering equipment”.

**Institutional Review Board Statement:** Not applicable.

**Informed Consent Statement:** Not applicable.

**Data Availability Statement:** Not applicable.

**Acknowledgments:** Not applicable.

**Conflicts of Interest:** The authors declare no conflict of interest.

### Abbreviations

|                    |  |
|--------------------|--|
| $c_p$              | specific heat;                                     |
| $g$                | gravitational acceleration;                        |
| $G$                | mass flowrate in the boundary layer;               |
| $h$                | heat transfer coefficient;                         |
| $k$                | thermal conductivity;                              |
| $m$                | mass;  |
| $M_i$              | molar mass;  |
| $n$                | number of moles;                                   |
| $p$                | pressure;  |
| $p_{cr}$           | critical pressure;                                 |
| $R$                | individual (specific) gas constant;                |
| $R_m$              | universal gas constant;                            |
| $T$                | temperature;                                       |
| $T_{cr}$           | critical temperature;                              |
| $u$                | streamwise velocity component;                     |
| $V$                | volume;  |
| $v$                | specific volume;                                   |
| $x$                | streamwise coordinate;                             |
| $y$                | spanwise (wall-orthogonal) coordinate;             |
| $\delta$           | boundary layer thickness;                          |
| $\mu$              | dynamic viscosity;                                 |
| $\rho$             | density;   |
| $Wa$               | van der Waals number;                              |
| $Z$                | compressibility factor                             |
| <i>Subscripts:</i> |  |
| 0                  | ideal gas;   |
| $m$                | average value;                                     |
| $w$                | value at the wall;                                 |
| $\infty$           | value at the outer boundary of the boundary layer. |

### References

1. Kormann, M.; Krüger, I.L. Application of a Real Gas Model by van der Waals for a Hydrogen Tank Filling Process. In Proceedings of the 13th International Modelica Conference, Regensburg, Germany, 4–6 March 2019; pp. 665–670. [\[CrossRef\]](#)
2. Beyer, C.; Oellrich, L.R. High Pressure Phase Equilibria of Copolymer Solutions—Experiments and Correlation. In *Supercritical Fluids as Solvents and Reaction Media*; Elsevier: Amsterdam, The Netherlands, 2004; Chapter 1.3; pp. 61–84. [\[CrossRef\]](#)
3. Çengel, Y.A.; Boles, M.A. *Thermodynamics: An Engineering Approach*, 5th ed.; McGraw-Hill Education: New York, NY, USA, 2004.
4. Baehr, H.-D.; Kabelac, S. *Thermodynamik: Grundlagen und Technische Anwendungen*, 15th ed.; Springer: Berlin/Heidelberg, Germany, 2012.
5. Weigand, B.; Köhler, J.; von Wolfersdorf, J. *Thermodynamik Kompakt*, 4th ed.; Springer: Berlin/Heidelberg, Germany, 2016.
6. Reid, R.C.; Prausnitz, J.M.; Poling, B.E. *The Properties of Gases and Liquids*, 4th ed.; McGraw-Hill: New York, NY, USA, 1987.
7. Eremin, V.V.; Kargov, S.I.; Kuzmenko, N.E. Real Gases. Equations of State, Thermodynamic Properties, Statistical Description. In *Methodical Guidelines for Students of Chemical Faculties of Universities*; Poltorak, O.M., Ed.; Chemical Faculty of Moscow State University: Moscow, Russia, 1998.
8. Avramenko, A.A.; Tyrinov, A.I.; Shevchuk, I.V.; Dmitrenko, N.P.; Kravchuk, A.V.; Shevchuk, V.I. Mixed convection in a vertical circular microchannel. *Int. J. Ther. Sci.* **2017**, *121*, 1–12. [\[CrossRef\]](#)
9. Avramenko, A.A.; Tyrinov, A.I.; Shevchuk, I.V.; Dmitrenko, N.P.; Kravchuk, A.V.; Shevchuk, V.I. Mixed convection in a vertical flat microchannel. *Int. J. Heat Mass Transf.* **2017**, *106*, 1164–1173. [\[CrossRef\]](#)
10. Vargas, M.; Sierra, F.Z.; Ramos, E.; Avramenko, A.A. Steady natural convection in a cylindrical cavity. *Int. Commun. Heat Mass Transfer* **2002**, *29*, 213–221. [\[CrossRef\]](#)
11. Gorbunov, A.A.; Nikitin, S.A.; Polezhaev, V.I. Conditions of Rayleigh-Bénard Convection Onset and Heat Transfer in a Near-Critical Medium. *Fluid Dyn.* **2007**, *42*, 704–718. [\[CrossRef\]](#)

12. Polezhaev, V.I.; Gorbunov, A.A.; Nikitin, S.A.; Soboleva, E.B. Numerical modelling of Rayleigh-Benard convection and heat transfer in normal  $^3\text{He}$  near the critical point. *J. Phys. Conf. Ser.* **2009**, *150*, 032083. [[CrossRef](#)]
13. Polezhaev, V.I.; Soboleva, E.B. Rayleigh-Benard Convection in a Near-Critical Fluid in the Neighborhood of the Stability Threshold. *Fluid Dyn.* **2005**, *40*, 209–220. [[CrossRef](#)]
14. Polezhaev, V.I.; Soboleva, E.B. Thermal gravity-driven convection of near-critical helium in enclosures. *Low Temp. Phys.* **2003**, *29*, 648–652. [[CrossRef](#)]
15. Teymourtasha, A.R.; Warkiani, M.E. Natural convection over a Non-Isothermal Vertical Plate in Supercritical Fluids. *Trans. B Mech. Eng.* **2009**, *16*, 470–478.
16. Accary, G.; Bontoux, P.; Zappoli, B. Turbulent Rayleigh-Bénard convection in a near-critical fluid by three-dimensional direct numerical simulation. *J. Fluid Mech.* **2009**, *619*, 127–145. [[CrossRef](#)]
17. Liu, J. Thermal Convection in the van der Waals Fluid. In *Frontiers in Computational Fluid-Structure Interaction and Flow Simulation*; Birkhäuser: Cham, Germany, 2018; pp. 377–398. [[CrossRef](#)]
18. Onuki, A. Dynamic van der Waals Theory of Two-Phase Fluids in Heat Flow. *Phys. Rev. Lett.* **2005**, *94*, 054501. [[CrossRef](#)] [[PubMed](#)]
19. Laurila, T.; Carlson, A.; Do-Quang, M.; Ala-Nissila, T.; Amberg, G. Thermohydrodynamics of boiling in a van der Waals fluid. *Phys. Rev. E* **2012**, *85*, 026320. [[CrossRef](#)] [[PubMed](#)]
20. Onuki, A. Dynamic van der Waals theory. *Phys. Rev. E* **2007**, *75*, 036304. [[CrossRef](#)] [[PubMed](#)]
21. Lamorgese, A.G.; Mauri, R. Diffuse-interface modeling of liquid-vapor phase separation in a van der Waals fluid. *Phys. Fluids* **2009**, *21*, 044107. [[CrossRef](#)]
22. Denniston, C.; Yeomans, J.M. Diffuse interface simulation of Marangoni convection. *Phys. Chem. Chem. Phys.* **1999**, *1*, 2157–2161. [[CrossRef](#)]
23. Ramazanov, M.M. Conditions for the Absence and Occurrence of Filtration Convection in a Compressible Gas. *J. Eng. Phys. Thermophys.* **2014**, *87*, 541–547. [[CrossRef](#)]
24. Soboleva, E.B. Adiabatic Heating and Convection in a Porous Medium Filled with a Near-Critical Fluid. In *Proceedings of the ITP2007 Interdisciplinary Transport Phenomena V: Fluid, Thermal, Biological, Materials and Space Sciences*, Bansko, Bulgaria, 14–19 October 2007.
25. Isachenko, V.P.; Osipova, V.A.; Sukomel, A.S. *Heat Transfer*; Mir Publishers: Moscow, Russia, 1980.